

Subtype-Dependence of NMDA Receptor Channel Open Probability

Nansheng Chen,¹ Tao Luo,¹ Lynn A. Raymond^{1,2,3}

¹Kinsmen Laboratory of Neurological Research, Department of Psychiatry, ²Department of Physiology, and ³Division of Neurology, Department of Medicine, University of British Columbia, Vancouver, British Columbia V6T 1Z3 Canada

NMDA receptor-mediated calcium transients play a critical role in synaptogenesis, synaptic plasticity, and excitotoxicity. NMDA receptors are heteromeric complexes of NR1A combined with NR2A, NR2B, NR2C, and/or NR2D subunits. The NR2 subunits determine a variety of electrophysiological and pharmacological properties of the NMDA receptor complex. In this report, we provide evidence for the first time that there is also a significant difference in peak channel open probability (P_o) between NMDA receptors composed of NR1A/NR2A and those of NR1A/NR2B subunits. First, whole-cell patch-clamp recordings from human embryonic kidney (HEK) 293 cells expressing NMDA receptors revealed that NR1A/NR2A-mediated peak current densities are approximately four times larger than those of NR1A/NR2B. We show that this fourfold difference is unlikely caused by differences in receptor surface expression,

since these levels were similar for the two subtypes by Western blot analysis. To determine whether P_o contributed to the difference in peak current densities, we used two different open channel antagonists, MK-801 and 9-aminoacridine, in a variety of experimental paradigms. Our results indicate that peak P_o is significantly higher (twofold to fivefold) for NR1A/NR2A than NR1A/NR2B, with estimated values of ~ 0.35 and 0.07 , respectively. These results suggest that a change in the relative expression levels of NR2A and NR2B can regulate peak amplitude of NMDA receptor-mediated excitatory postsynaptic potentials and therefore may play a role in mechanisms underlying synaptic plasticity.

Key words: patch-clamp recording; transient transfection; recombinant receptors; use-dependent block; tail current; charge transfer

NMDA receptors have been the focus of extensive investigation because of their central role in a number of physiological processes, such as synaptogenesis and synaptic plasticity, as well as pathological conditions, including Huntington's disease and ischemic stroke (for review, see Chen et al., 1999; Dingledine et al., 1999). Recent evidence indicates NMDA receptors are heteromeric complexes of NR1A and the NR2A-NR2D subunits, resulting in a tetrameric or pentameric complex (Dingledine et al., 1999). Heterologous expression of NR1A with any one of the NR2 subunits yields a recombinant receptor with remarkably unique pharmacological and biophysical properties (Sucher et al., 1996). Since NR2 subunit expression varies across different brain regions and neuronal types, as well as with developmental stage (Monyer et al., 1994; Sheng et al., 1994), function and modulation of NMDA receptors are highly regulated both spatially and temporally.

A key determinant of the amplitude and spatial distribution of NMDA receptor-mediated calcium transients is the channel open probability (P_o). Interestingly, this channel property has been shown to be modified by a variety of physiological processes, including phosphorylation/dephosphorylation (Kohr and Seeburg, 1996; Wang et al., 1996; Lu et al., 1998), the polymerization state of the actin cytoskeleton (Rosenmund and Westbrook, 1993), and receptor interactions with calcium/calmodulin (Ehlers et al.,

1996; Zhang et al., 1998; Krupp et al., 1999). In addition, P_o can be altered by extracellular agents that reduce or oxidize the disulfide bonds of the receptor (Brimecombe et al., 1997). However, in each of these reports, P_o measurements were relative, and no absolute numbers were given because of the difficulty in determining the number of channels in the membrane during single-channel recording.

Huettnner and Bean (1988) were the first to report a quantitative value for neuronal NMDA receptor P_o . They used MK-801, a slowly reversible open channel antagonist, to determine a P_o of 0.002 from whole-cell recordings of NMDA-evoked currents in cultured rat neocortical neurons. However, subsequent studies using MK-801 have reported widely differing results for P_o , up to as high as 0.3 (Jahr, 1992; Hessler et al., 1993; Rosenmund et al., 1993, 1995). Dzubay and Jahr (1996) have argued that some of this variability may be attributable to differences in experimental preparation and protocol, which may affect NMDA receptor inactivation. As well, two studies have shown that measurements of neuronal NMDA receptor P_o made from recordings in the outside-out patch mode are significantly larger than those made in the whole-cell mode (Benveniste and Mayer, 1995; Rosenmund et al., 1995).

We propose that NMDA receptor subunit composition may play an important role in determining P_o . To test this idea, we assessed the relative P_o for NR1A/NR2A and NR1A/NR2B expressed in human embryonic kidney (HEK) 293 cells. Because we observed a fourfold difference in peak macroscopic whole-cell current between these receptor subtypes, our experimental protocols and data analysis were designed to assess P_o at the peak of the current response (i.e., maximal P_o) in the whole-cell recording mode. From our results we conclude that peak P_o for NR1A/NR2A is twofold to fivefold higher than that for NR1A/NR2B.

Received Jan. 19, 1999; revised May 26, 1999; accepted June 1, 1999.

This work was supported by a grant from the Medical Research Council (MRC) (L.A.R.). N.C. was supported by a fellowship from the Huntington's Disease Society of America. L.A.R. is an MRC (Canada) Scholar. We thank Drs. T. H. Murphy and C. J. Price for useful discussions and suggestions, and Moira Thejomayen for assistance in manuscript preparation.

Correspondence should be addressed to Dr. Lynn A. Raymond, Division of Neuroscience, Department of Psychiatry, University of British Columbia, 4N3-2255 Wesbrook Mall Vancouver, BC, Canada V6T 1Z3.

Copyright © 1999 Society for Neuroscience 0270-6474/99/196844-11\$05.00/0

MATERIALS AND METHODS

Cell culture and transfection. Culture and transfection of HEK 293 cells (CRL 1573; ATCC, Rockville, MD) were as described previously (Chen et al., 1997). Briefly, HEK 293 cells were routinely maintained in incubators set at 37°C and 5% CO₂, with culture media prepared from minimum essential medium (Life Technologies, Burlington, Ontario, Canada), containing Earle's salts (Life Technologies), supplemented with 2 mM L-glutamine, 1 mM sodium pyruvate (Life Technologies), 100 U/ml penicillin/streptomycin (Life Technologies), and 10% fetal bovine serum (Hyclone, Logan, UT). Cells were passaged once every 2–4 d. For calcium phosphate transfection (Chen and Okayama, 1987), cells were plated at a density of 1×10^6 cells/ml in 10 cm culture dishes (Falcon; Becton Dickinson, Franklin Lakes, NJ). For the purpose of this project, cells were transfected with cDNAs encoding NR1A [a gift from Dr. S. Nakanishi, Kyoto University, Kyoto, Japan; nomenclature of Sugihara et al. (1992); also known as NR1A-1a (Hollmann et al., 1993)], NR2A (from mouse brain, also called $\epsilon 1$, a gift from Dr. M. Mishina, University of Tokyo, Tokyo, Japan) or NR2B (from Dr. S. Nakanishi), and β -galactosidase (β -gal) at a ratio of 1:1:1. A total of 12 μ g of plasmid cDNA was used for transfection of a 10 cm culture plate. The transfection efficiency was assessed using the β -gal staining procedure (Raymond et al., 1996). HEK 293 cells were transfected for ~8 hr in a 3% CO₂ incubator. After transfection, 1 mM (\pm)-2-amino-5-phosphonopentanoic acid (APV; Research Biochemicals, Natick, MA) and/or 100 μ M memantine (Research Biochemicals) were added to the culture media, and the cells were transferred onto glass coverslips in 35 mm culture plates (Falcon). For Western blot analysis, cells were replated in 10 cm culture dishes precoated with 10 μ g/ml poly-D-lysine.

Electrophysiology. The whole-cell patch clamp recording technique and recording solutions were essentially the same as previously described (Chen et al., 1997). At 24–36 hr after the start of transfection, the cells were transferred from 35 mm culture plates (Falcon) to the recording chamber on the stage of an inverted microscope (Axiocvert 100; Carl Zeiss, Thornburg, NY). Agonist-evoked currents were recorded in the whole-cell mode under voltage clamp ($V_H = -60$ mV). Recording pipettes were pulled from borosilicate glass (Warner Instruments, Hamden, CT) with the Narishige (Tokyo, Japan) PP-83 electrode puller. Electrodes with open tip resistances of 1–5 M Ω were used. After establishing the whole-cell mode, cells were lifted from the coverslip. Ultrafast application of agonists was achieved by a piezo-driven θ -tube (Hilgenburg, Malsfeld, Germany) (see also, Chen et al., 1997). Control and agonist solutions were continuously gravity-fed through the two sides of the θ -tube. The 10–90% rise time for solution exchange was 0.5–0.8 msec (Fig. 1A₁) at the open tip of a recording electrode and 3.0–3.9 msec (Fig. 1A₂) for the whole-cell response, as measured by jumps between NaCl- and N-methylglutamine (NMG)-containing extracellular recording solutions. Extracellular recording solution contained (in mM) 145 NaCl, 5.4 KCl, 0.2 CaCl₂, 11 glucose, and 10 HEPES, titrated to pH 7.35 with 10 M NaOH. In all experiments, 50 μ M glycine was added to both control and glutamate-containing extracellular solutions. Glutamate, glycine, MK-801 (Research Biochemicals), and 9-aminoacridine (Aldrich, Milwaukee, WI) stock solutions were stored at –20°C; aliquots were thawed on ice for each day's experiment and diluted into the extracellular recording solution just before use. The intracellular recording solution contained (in mM) 145 KCl, 5.5 1,2-bis(2-aminophenoxy)ethane-*N,N,N',N'*-tetra-acetic acid, 4 MgATP, and 10 HEPES, titrated to pH 7.25 with KOH. Currents were sampled at 2 kHz and acquired and analyzed using pClamp software and the Axopatch 200A amplifier (Axon Instruments, Foster City, CA). Current amplitude measurement and kinetics fitting were conducted with Clampfit software.

Western blot analysis. The analyses of overall NMDA receptor expression level and surface expression level were carried out essentially as described in Chen et al. (1999). HEK 293 cells transfected with NR1A/NR2A or NR1A/NR2B were washed twice with warm PBS and incubated with the membrane-impermeable reagent N-hydroxysuccinimide-SS-biotin (NHS-SS-biotin; Pierce, Rockford, IL) at a concentration of 1.5 mg/ml in PBS containing Mg²⁺/Ca²⁺ for 30 min at 4°C with mild shaking. The cells were washed twice with Mg²⁺/Ca²⁺-containing PBS supplemented with 100 mM glycine, and incubated with this solution for 30 min in order to remove any NHS-SS-biotin not bound to protein. After washing the cells with Mg²⁺/Ca²⁺-containing PBS three times, cells were scraped with 1 ml of ice-cold harvest buffer (1 mM EGTA, 1 mM EDTA, 1 mM phenylmethylsulfonyl fluoride, and 100 U/ml aprotinin in PBS) into eppendorf tubes prechilled on ice, sonicated (10 sec), and centrifuged (14,000 rpm for 30 min at 4°C). The precipitates, which

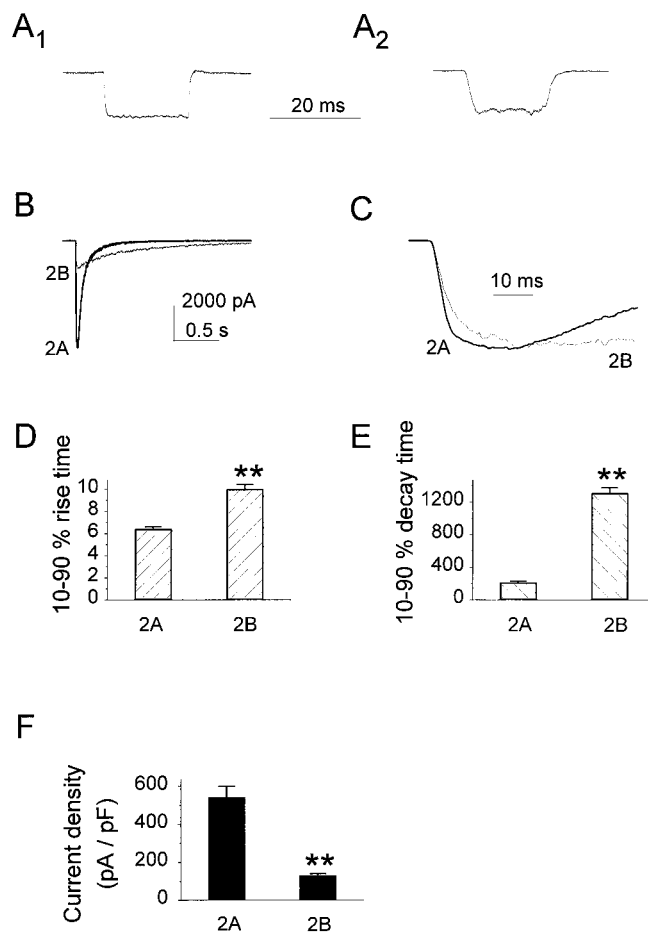


Figure 1. Peak current density of agonist-evoked responses is larger for recordings from cells transfected with NR1A/NR2A than NR1A/NR2B. A₁, A₂, Representative traces of open tip recording (A₁) or whole-cell current (A₂) made by switching between NMG-containing and NaCl-containing extracellular solutions. B, Representative current traces in response to 20 msec application of 1 mM glutamate (in continuous presence of 50 μ M glycine) recorded from a cell transfected with either NR1A/NR2A (thick line) or NR1A/NR2B (thin line). C, NR1A/NR2B current trace (thin line) normalized to the peak of an NR1A/NR2A current trace (thick line) to illustrate difference in activation time courses. D, Bars show mean \pm SEM for 10–90% rise-time ($n = 10$ for both subtypes; ** $p < 0.01$ by unpaired t test). E, Mean \pm SEM for 10–90% decay time ($n = 10$ for both subtypes; ** $p < 0.01$ by unpaired t test). F, Bars indicate mean \pm SEM for current responses to 100 μ M glutamate (in the continuous presence of 50 μ M glycine) recorded from $n = 60$ (NR1A/NR2A) or $n = 106$ (NR1A/NR2B) different cells. ** $p < 0.001$ by unpaired t test.

correspond to the membrane fraction, were redissolved by sonication (10 sec) in solubilization buffer (harvest buffer with 1% Triton X-100) followed by end-over-end mixing for 30 min in 4°C cold room. After centrifugation (14,000 rpm, 30 min at 4°C), supernatants were saved and stored at –80°C for further analysis. Protein concentrations were determined by bicinchoninic acid protein assay (BCA kit; Pierce).

For analysis of NMDA receptor overall expression, identical amounts (1, 2, and 4 μ g) of protein from the membrane fraction of each cell lysate were loaded to 8% SDS-PAGE. For the assessment of surface receptor expression level, the remainder of each cell lysate was incubated with 100 μ l (spun down from 200 μ l suspension) neutravidin-linked beads (Pierce) by end-over-end rotation for 2 hr at 4°C. Beads were extensively centrifuged and washed to isolate bead-bound proteins. These proteins were eluted by incubating the beads with dithiothreitol-containing SDS-PAGE loading buffer and loaded to 8% SDS-PAGE.

After overnight transfer of gels to PVDF membranes, the membranes

were blotted with anti-NR1A polyclonal antibodies (Upstate Biotechnology, Lake Placid, NY) at 1 μ g/ml concentration. The membranes were then incubated with horseradish peroxidase-conjugated donkey anti-rabbit secondary antibody (Amersham, Arlington Heights, IL) diluted 1:5000. Bands were visualized by enhanced chemiluminescence (ECL; Amersham). Band intensities were determined by densitometry, and protein quantity-band density relation standard curves were generated from measurements of bands representing the 1, 2, and 4 μ g aliquots of the total membrane lysates. Surface protein expression level was calculated as a percentage of total membrane protein.

Materials. All chemicals, unless otherwise stated, were purchased from Sigma (St. Louis, MO).

Data analysis and presentation. Results were presented as mean \pm SEM. Different sets of results were compared using the Student's *t* test. Significant differences were determined at 95% confidence intervals. Figures were created with Origin or Photoshop software.

RESULTS

To determine the relative channel open probability of NMDA receptor subtypes, we have compared macroscopic currents recorded from HEK 293 cells transfected with either NR1A/NR2A or NR1A/NR2B. We chose to study peak P_o using the whole-cell recording mode because this configuration preserves the integrity of cytoskeleton and membrane-associated proteins better than the outside-out patch mode, and therefore may better reflect the physiological state. Moreover, ultrafast superfusion of agonists and antagonists can be achieved for whole-cell recordings from HEK 293 cells by lifting cells from the chamber floor to within 100 μ m of the openings of the piezo-controlled application θ -tube (see Materials and Methods; exchange time at the open tip of a recording electrode is illustrated in Fig. 1A). The relation between the macroscopic NMDA receptor-mediated peak current amplitude (I_{peak}) and peak P_o is given by:

therefore,

$$I_{\text{peak}} = i \cdot N \cdot P_o \quad (1)$$

$$P_o = (1/i) \cdot I_{\text{peak}}/N \quad (2)$$

where i is the unitary current and N is the number of functional surface receptors. Single-channel conductances have been shown to be identical (with a main conductance of 50 pS and a subconductance of 38 pS) for these two subtypes of NMDA receptors expressed in HEK 293 cells (Stern et al., 1992, 1995). Therefore, if relative I_{peak} and N are measured, then the relative P_o can be determined.

Macroscopic currents mediated by NR1A/NR2A are significantly larger than those of NR1A/NR2B

After transient transfection with either NR1A/NR2A or NR1A/NR2B, whole-cell currents were recorded under voltage-clamp (−60 mV) from HEK 293 cells in response to brief (20 msec) applications of a saturating concentration of agonist (Fig. 1B). As described previously (Monyer et al., 1992, 1994; McBain and Mayer, 1994; Vicini et al., 1998; Chen et al., 1999), NR1A/NR2A and NR1A/NR2B mediate currents with dramatic kinetic differences. The 10–90% rise time was significantly slower for NR1A/NR2B- than NR1A/NR2A-mediated currents, although this difference was small (6.4 ± 0.2 msec, $n = 10$ for NR1A/NR2A; 10.0 ± 0.4 msec, $n = 10$ for NR1A/NR2B; $p < 0.01$ by unpaired *t* test; Fig. 1C,D). As well, the time courses of desensitization, inactivation, and deactivation of NR1A/NR2A currents were significantly faster than those of NR1A/NR2B (Krupp et al., 1996; Chen et al., 1997, 1999; see Fig. 1B,E for deactivation). Interestingly, mean peak current amplitude was approximately fourfold

larger for NR1A/NR2A-transfected cells (data not shown). Because cell surface membrane area can affect numbers of surface receptors, we normalized peak current amplitude to cell capacitance (current density, picoamperes per picofarads). Mean peak current density was also approximately fourfold larger for NR1A/NR2A-transfected cells (Fig. 1F; 543 ± 56 pA/pF, $n = 60$ for NR1A/NR2A vs 130 ± 9 pA/pF, $n = 106$ for NR1A/NR2B; $p \ll 0.01$, unpaired *t* test). Therefore, the ratio of mean I_{peak} for NR1A/NR2A to that for NR1A/NR2B was ~ 4 . Based on this ratio, we reasoned that peak channel open probability and/or receptor surface expression level must be significantly higher for NR1A/NR2A than NR1A/NR2B.

NR1A/NR2A- and NR1A/NR2B-transfected cells show similar total and surface expression of NR1A

To investigate the relative mean numbers of surface receptors for NR1A/NR2A- and NR1A/NR2B-transfected cells, we compared total and surface expression of these receptors in the membrane fraction of transfected HEK 293 cell lysates by Western blot analysis. Assuming that the two subtypes share identical stoichiometry (see Discussion), we used anti-NR1A polyclonal antibodies to probe the expression of both NR1A/NR2A and NR1A/NR2B. Figure 2 shows representative Western blots and the pooled data from four different experiments. Although total expression of NR1A was approximately twofold higher in NR1A/NR2B- than NR1A/NR2A-transfected cells (Fig. 2A,C), the fraction of NR1A expressed at the cell surface was twofold higher for NR1A/NR2A-transfected cells (Fig. 2A,B). Thus, relative NR1A surface expression levels for these two subtypes were not significantly different (Fig. 2D; $p = 0.12$, paired *t* test). Assuming that NR1A expression levels accurately reflect numbers of NR1A/NR2A and NR1A/NR2B receptors (see Discussion), then mean numbers of surface receptors for NR1A/NR2A- and NR1A/NR2B-transfected cells were very similar. These data taken together with the results from analysis of peak macroscopic current densities suggested that P_o (NR1A/NR2A)/ P_o (NR1A/NR2B) should be approximately 4. In order to test this conclusion more directly, we examined the relative peak P_o of NR1A/NR2A and NR1A/NR2B using two use-dependent antagonists: MK-801 and 9-aminoacridine.

MK-801 block indicates peak P_o is significantly larger for NR1A/NR2A than NR1A/NR2B

MK-801 is a NMDA receptor open channel blocker that is irreversible on a time scale of tens of minutes at hyperpolarized potentials, making it a useful tool for estimating P_o (Huettner and Bean, 1988; Jahr, 1992; Rosenmund et al., 1995; Dzuby and Jahr, 1996). Therefore, we recorded whole-cell NMDA receptor-mediated currents from transfected HEK 293 cells in the absence and presence of MK-801. For these experiments, the extracellular solution contained reduced calcium (0.2 mM) in order to minimize calcium-dependent inactivation and rundown (Jahr 1992; Legendre et al., 1993; Rosenmund and Westbrook, 1993; Ehlers et al., 1996; Krupp et al., 1998; Zhang et al., 1998; Price et al., 1999). As mentioned earlier, a 20 msec agonist pulse (1 mM glutamate and 50 μ M glycine) evoked a fast inward current, with a 10–90% rise-time < 10 msec, which deactivated rapidly (although this decay phase was considerably slower for NR1A/NR2B; Fig. 1B,E). Such a protocol was applied every 20 sec until the peak current amplitude was stable, as defined by at least five consecutive current responses with less than $\pm 2\%$ variability in peak amplitude. Then, following a protocol used by Jahr (1992),

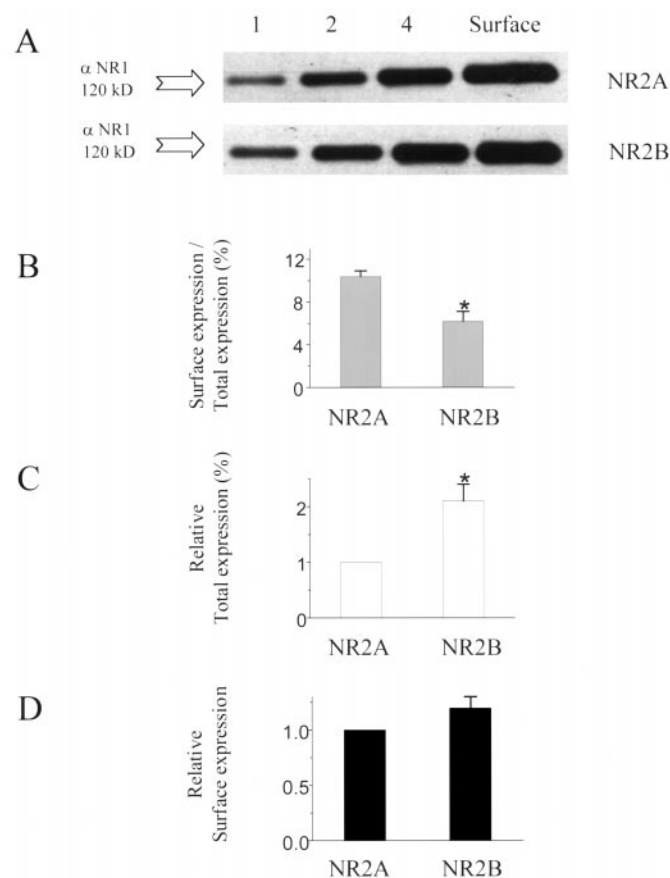


Figure 2. Cells transfected with NR1A/NR2A or NR1A/NR2B show similar levels of NR1A surface expression. *A*, Representative Western blot of membrane fraction of lysates from NR1A/NR2A- and NR1A/NR2B-transfected cells probed with anti-NR1A antibody. 1, 2, and 4 represent micrograms of protein loaded in each lane; Surface represents neutravidin bead-precipitated receptors. *B–D*, Band intensities from Western blots were analyzed by densitometry, and bars represent mean \pm SEM from $n = 4$ experiments. In *B*, the fraction of total NR1A protein expressed at the cell surface in each experiment was calculated by comparing “surface” band intensity to band intensities in lanes loaded with total membrane protein (1, 2, and 4). * $p < 0.05$ by unpaired t test. In *C*, band intensities measured for lanes 1, 2, and 4 of NR1A/NR2B cell lysates in each experiment were normalized to the values measured for lanes loaded with equal amounts of membrane protein from NR1A/NR2A-transfected cells. * $p < 0.05$ by paired t test. In *D*, the fraction of total NR1A/NR2B expressed at the cell surface in each experiment (see *B*) was normalized for the difference in relative total receptor expression of NR1A/NR2A and NR1A/NR2B (see *C*).

20 μ M MK-801 was added to both the control and agonist solutions, and a single agonist-evoked response was recorded [Fig. 3*A*₂, trace *b*, *B*₂, trace *b*; peak amplitude of trace *b* was normalized to the control response (trace *a*)] before removing MK-801 from all solutions. For both NR1A/NR2A and NR1A/NR2B, ~60% of the peak current was blocked in the presence of an equilibrium concentration (20 μ M) of MK-801 (Fig. 3*D*), consistent with similar on-rates for MK-801 for these two subtypes. Note also that for both subtypes, the time courses of decay and charge transfer in the presence of MK-801 (Fig. 3*A*₂*B*₂, traces *b*, *Sb*, respectively) were markedly faster than in the absence of MK-801 (Fig. 3*A*₂*B*₂, traces *a*, *Sa*, respectively), indicating that MK-801 blocked the currents not only during the peak but also during deactivation. After extensive wash-out (2 min) of MK-801, subsequent applications of agonist elicited currents with smaller

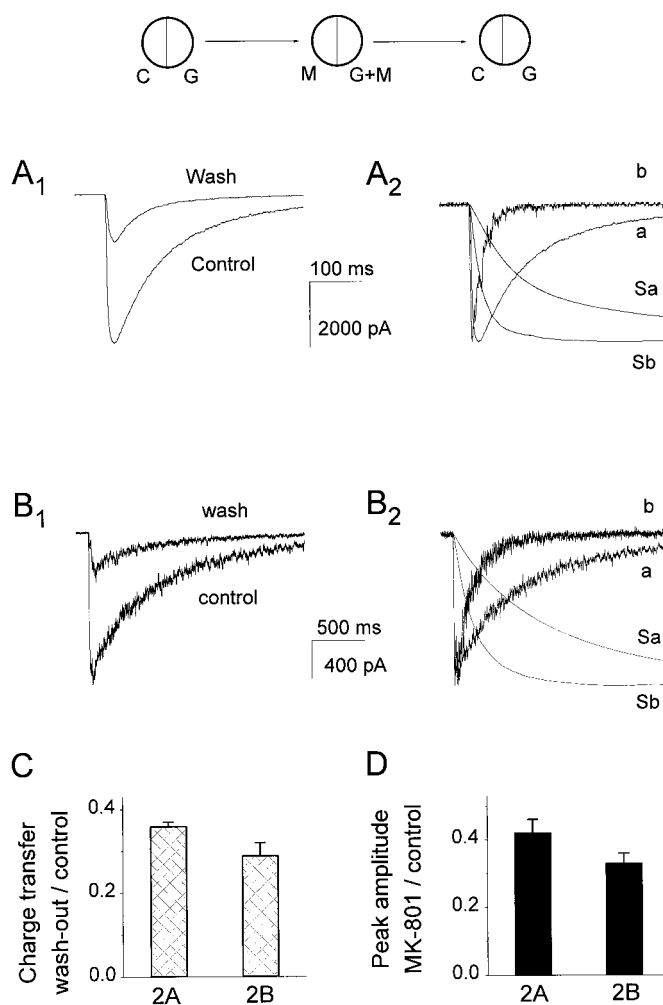


Figure 3. Peak current and decay phase attenuated in continuous presence of MK-801. *A*₁, *B*₁, Agonist-evoked current before (Control) and after (Wash) the application of 20 μ M MK-801 in both agonist and control solutions, recorded from an NR1A/NR2A (*A*₁) or an NR1A/NR2B (*B*₁) transfected cell under voltage-clamp configuration (−60 mV). *A*₂, *B*₂, Agonist-evoked current in the absence (trace *a*) or in the presence (trace *b*) of MK-801 in both solutions was recorded from an NR1A/NR2A (*A*₂) or an NR1A/NR2B (*B*₂) transfected cell. Peak current in the presence of MK-801 (*b*) was normalized to that in the absence of antagonist (*a*). Cumulative charge transfer time course curves (trace *Sa* and trace *Sb*) were obtained by integrating corresponding traces (*a* and *b*, respectively) over time. Fifty micromolar glycine was included in all solutions. *C*, Bars show mean \pm SEM for fraction of total charge transfer remaining after wash-out of 20 μ M MK801 ($n = 5$ for NR1A/NR2A and $n = 6$ for NR1A/NR2B; $p = 0.23$, unpaired t test). *D*, Mean \pm SEM for peak current measured in the presence of MK-801 normalized to that measured under control conditions ($n = 4$ for both subtypes; $p = 0.15$ by unpaired t test). The circles at the top of the figure illustrate the tip of the piezo-driven θ tube (see Materials and Methods) and the solutions used for recording: C, Control; G, 1 mM glutamate; M, MK-801. Extracellular solution contained 0.2 mM calcium.

amplitudes but similar time courses, compared to the pre-MK-801 responses (Fig. 3*A*₁, *B*₁) as also observed by Jahr (1992). After wash-out of 20 μ M MK-801, both the peak and the charge transfer in response to a single application of saturated agonist showed a decrease of ~70% compared to the control response for both subtypes (for NR1A/NR2A, $64 \pm 1\%$, $n = 4$; for NR1A/NR2B, $71 \pm 3\%$, $n = 4$, $p = 0.25$, unpaired t test; Fig. 3*A*₂, *B*₂, *C*). These results are similar to those found for neuronal NMDA receptors

A NR1A / NR2A

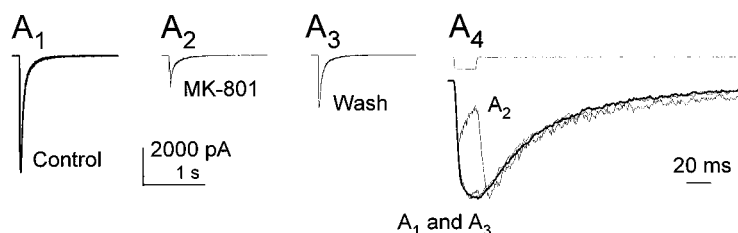
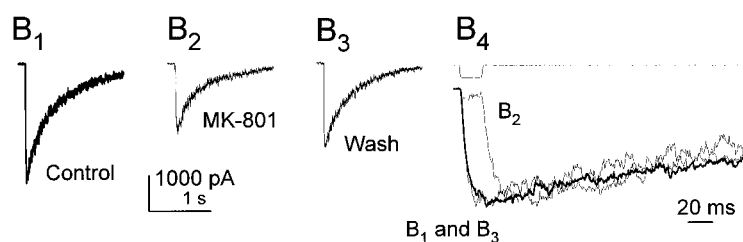


Figure 4. Brief pulse of 200 μM MK-801, applied together with glutamate, attenuates only the peak NMDA receptor-mediated current response. Recordings made from representative cells expressing NR1A/NR2A (*A*) or NR1A/NR2B (*B*). After establishing a stable current response to 20 msec application of 1 mM glutamate alone (*A*₁, *B*₁, *Control*), 200 μM MK-801 was added to agonist solution, and a single response was recorded (*A*₂, *B*₂, *MK-801*). The glutamate-evoked current response recorded after extensive wash-out of MK-801 is shown in *A*₃ and *B*₃ (*Wash*). Normalized current traces shown on expanded time scale in *A*₄ and *B*₄ illustrate that the decay phases of the control (thick line), MK-801, and wash (both shown as *thin lines*) traces all follow the same time course; open tip recordings for these experiments are shown above traces. Extracellular solution contained 0.2 mM calcium.

B NR1A / NR2B



(Jahr, 1992) and indicate that total P_o for the peak plus the deactivation phase of the current response is similar for the two subtypes.

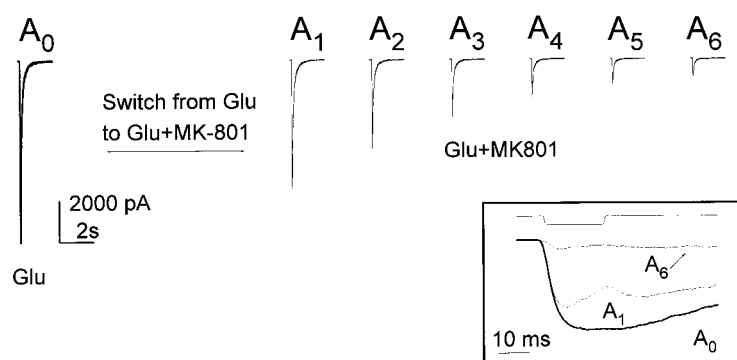
To estimate P_o for the peak current, we followed the analysis used by Jahr (1992). Since the peak current response occurred during the 20 msec agonist application, after which current decayed, we measured the fraction of total charge transfer occurring within this 20 msec period. In the presence of 20 μM MK-801, ~55% of the charge transfer occurred within 20 msec after the beginning of agonist application for NR1A/NR2A, whereas only 10% of the charge transfer occurred in this time period for NR1A/NR2B (Fig. 3*A*₂, traces *b*, *Sb*; *B*₂, traces *b*, *Sb*; $n = 4$). Increasing the MK-801 concentration above 20 μM did not result in any increase in charge transfer during the 20 msec agonist application (data not shown), as also reported by Jahr (1992). Thus, we estimate that peak P_o for NR1A/NR2A is 0.35 ($= 0.64 \times 0.55$), whereas peak P_o for NR1A/NR2B is approximately fivefold smaller at 0.07 ($= 0.71 \times 0.10$).

As an alternate approach for obtaining information on peak open probability, we used a protocol in which MK-801 had access to open channels only during the peak of the agonist-evoked current response. As before, we recorded macroscopic current evoked by brief applications (20 msec) of saturating agonist from HEK 293 cells transfected with NR1A/NR2A or NR1A/NR2B. After establishing a stable peak current response to glutamate alone (pulses applied at 20 sec intervals), MK-801 was added to the agonist solution, and 20 msec pulses of agonist and MK-801 were applied simultaneously. Figure 4 shows the results of this protocol using a single application of 200 μM MK-801 and illustrates three points. First, for both subtypes, 80–90% of the peak current response was blocked, and the rise-time to peak was attenuated significantly in the presence of 200 μM MK-801; however, the time courses for decay of the current responses with off-set of the MK-801/agonist pulse were identical to those observed for the control response (Fig. 4*A*₄, *B*₄; peak responses during and after MK-801 application were normalized to that of the control response). These results indicate that currents were

affected by MK-801 only during the 20 msec pulse (peak response) and not during the deactivation phase. Second, a “tail” current was observed with removal of glutamate and MK-801 (Fig. 4*A*₂, *B*₂; shown at higher gain in *A*₄, *B*₄). The rise-time for this tail current was similar to the rise-time of the control current response to rapid application of glutamate alone, consistent with opening of agonist-bound channels that had escaped MK-801 block during the 20 msec application. Third, the agonist-evoked response after wash-out of MK-801 was markedly larger than that observed for the previous protocol (Fig. 4*A*₃, *B*₃), consistent with the fact that only channels open during the peak response were blocked, but those opening during the deactivation phase were spared. Interestingly, when compared with the control response, the peak amplitude of the tail current with offset of the MK-801/agonist pulse, as well as the residual agonist-evoked response after wash-out of MK-801, were clearly larger for NR1A/NR2B than NR1A/NR2A (Fig. 4*A*_{1–3}, *B*_{1–3}).

To quantitate the effects of MK-801 block on the peak response, we used the protocol described for Figure 4 (see above) to measure progressive attenuation of peak current amplitude with repeated applications of agonist plus 20 μM MK-801 (Fig. 5). The peak amplitude of the tail current response was taken as a measure of the residual peak response to glutamate after each MK-801 application. As illustrated in Figure 5, glutamate-evoked peak amplitude attenuation was only ~30% for both subtypes (see insets), in contrast to the ~60% seen with glutamate application in the presence of an equilibrium concentration of 20 μM MK-801 (Fig. 3*D*); the decreased block of peak current with nonequilibrium application of 20 μM MK-801 reflects the solution exchange time over the whole cell. However, it is interesting to note that progressive attenuation of peak NR1A/NR2A current proceeded at a significantly faster rate than block of NR1A/NR2B peak current. Progressive block over several episodes (20 sec intervals) was fit well by a single exponential function (Fig. 6*A*, *C*), with a mean decay constant (in episodes) of 2.4 ± 0.2 for NR1A/NR2A and 8.1 ± 0.7 for NR1A/NR2B ($n = 8$ and 11

A NR1A / NR2A



B NR1A / NR2B

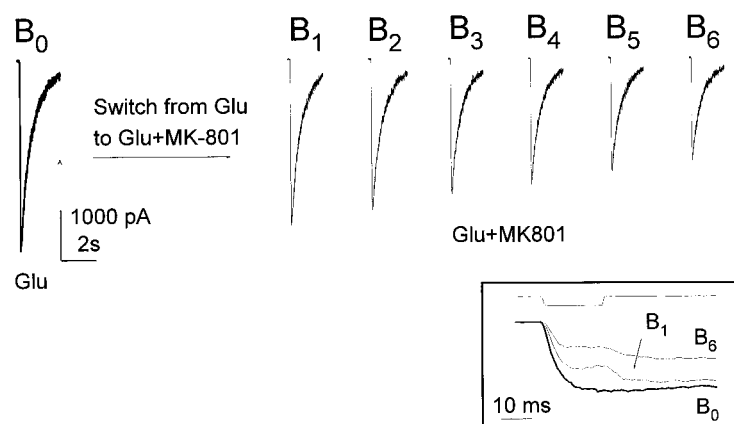


Figure 5. Representative current traces showing progressive attenuation of peak glutamate-evoked currents by 20 μ M MK-801 present only in agonist solution. Recordings were made in the continuous presence of 50 μ M glycine from a cell transfected with NR1A/NR2A (*A*) or NR1A/NR2B (*B*). A_0, B_0 , Representative control responses to 20 msec application of 1 mM glutamate alone. A_1 – A_6, B_1 – B_6 , Successive current responses to simultaneous application of 1 mM glutamate and 20 μ M MK-801 for 20 msec at 20 sec intervals. *Insets* show selected traces on an expanded time scale, along with the open tip recording to indicate speed of solution exchange in these experiments. Extracellular solution contained 0.2 mM calcium.

different cells, respectively). Consistent with a monoexponential function, the ratio of the amplitude of each successive peak (I_N) to that of the previous peak (I_{N-1}) was stable (Figs. 5, 6*B,D*), and mean values for this measure were significantly larger for NR1A/NR2B than NR1A/NR2A (Fig. 6*E*). In fact, the fraction of peak current blocked with each successive pulse ($1 - [I_N/I_{N-1}]$) was approximately threefold higher for NR1A/NR2A than for NR1A/NR2B ($0.28 \pm 0.02, n = 8$ vs $0.09 \pm 0.02, n = 11$, respectively; $p < 0.01$ by unpaired t test; Fig. 6*F*). If a difference in MK-801 on-rate accounted for the difference in time course of progressive MK-801 block, then the time courses for the two subtypes should become identical at sufficiently high MK-801 concentrations. Therefore, we compared progressive block of NR1A/NR2A and NR1A/NR2B currents by 10, 20, 50, 100, and 150 μ M MK-801. As expected, we observed a higher rate of block with increased MK-801 concentration, but this reached a maximum for both NR1A/NR2A and NR1A/NR2B at MK-801 concentrations $> 50 \mu$ M (Fig. 6*F*). Importantly, the ratio of the mean value of $1 - [I_N/I_{N-1}]$ for NR1A/NR2A to that of NR1A/NR2B remained significantly different at all five concentrations of MK-801 (3.2, 3.1, 2.6, 2.2, and 2.1 for 10, 20, 50, 100, 150 μ M, respectively). Together with data shown in Figure 3*D* suggesting that MK-801 on-rates are similar for the two subtypes, these data are consistent with the conclusion that the difference in time course of progression of MK-801 block can be attributed mainly to a significant difference in peak P_o .

9-Aminoacridine block demonstrates a larger fraction of channels open after the peak for NR1A/NR2B than for NR1A/NR2A

Results of the experiments with MK-801 indicate that total P_o (for the peak and deactivation phase of the macroscopic current response) is similar for NR1A/NR2A and NR1A/NR2B, but that maximal (or peak) P_o is at least twofold to threefold higher for NR1A/NR2A. These results suggest that the mean open time or opening frequency is smaller, and/or the distribution of latencies to first opening is shifted to longer times for NR1A/NR2B channels. We used the use-dependent antagonist 9-aminoacridine (9-AA) to address this issue more directly. As shown in Figure 7, *A* and *B*, brief (20 msec) coapplication of 100 μ M 9-AA and a saturating concentration of agonist (1 mM glutamate with 50 μ M glycine) resulted in 80–90% block of peak current, followed by a tail current after removal of agonist/9-AA. As for experiments with MK-801 (Fig. 4), the rise-time of the tail current was similar to that for current activation in response to agonist alone and likely represented opening of agonist-bound channels that had escaped block (see also Benveniste and Mayer, 1995). Also like the results with 200 μ M MK-801, the amplitude of the tail current relative to the control response was much larger for NR1A/NR2B than for NR1A/NR2A, indicating that a larger proportion of channels opened for the first time after the peak for NR1A/NR2B.

Unlike MK-801, block of open channels by 9-AA is reversible

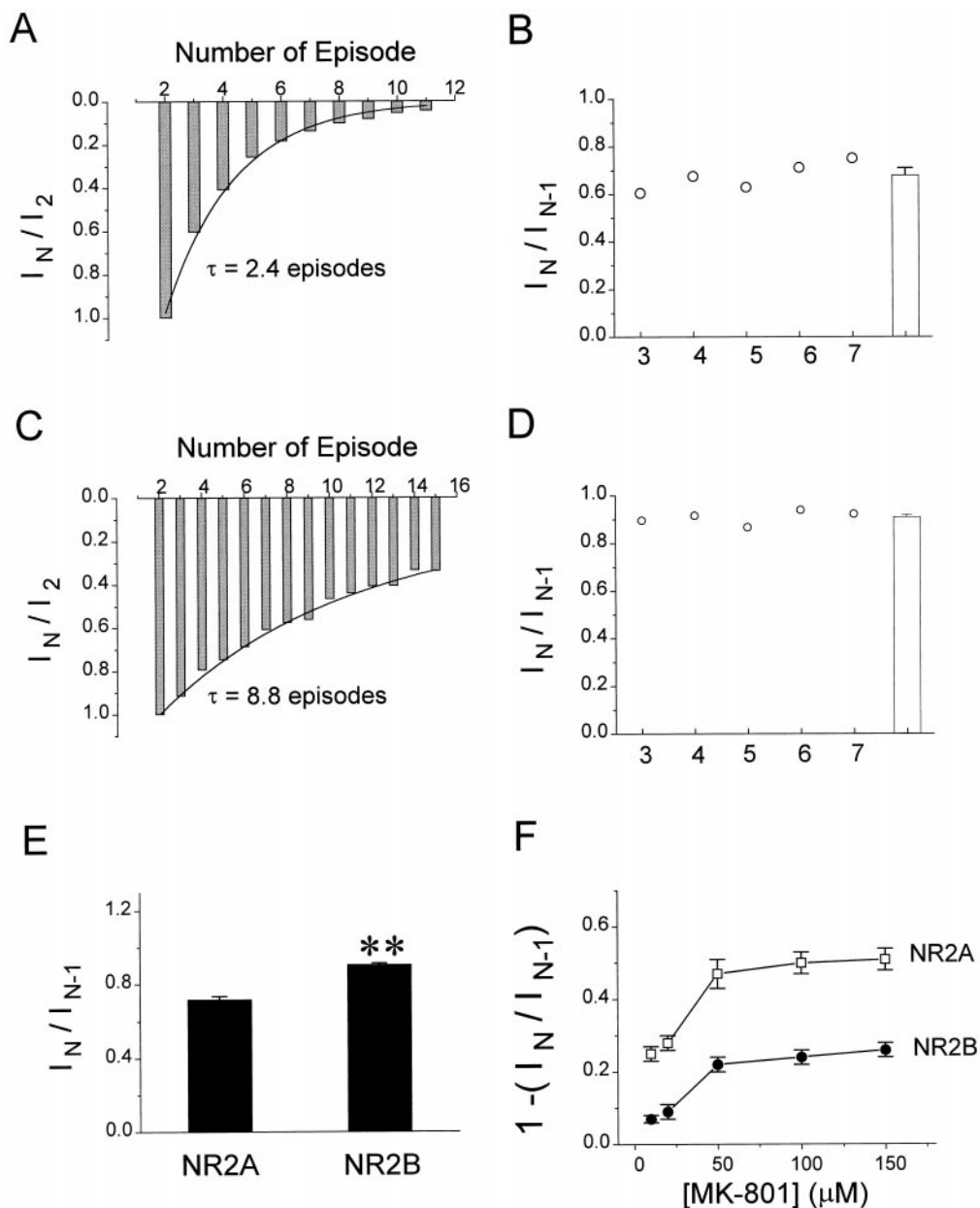


Figure 6. Progressive block by MK-801 of peak glutamate-evoked current is more rapid for NR1A/NR2A than NR1A/NR2B. *A–D*, Graphic representation of progressive MK-801 block in recordings from cell transfected with NR1A/NR2A (*A, B*) or NR1A/NR2B (*C, D*). *A, C*, Peak current amplitude measured with each successive pulse of glutamate plus MK-801 was normalized to the peak current response to the second application of 1 mM glutamate plus MK-801. Decay of peak current was fit by a single exponential function. *B, D*, Peak current amplitude recorded in response to each successive pulse of glutamate plus MK-801 (I_N) was normalized to peak current amplitude recorded in response to the previous glutamate plus MK-801 pulse (I_{N-1}). The mean ratio (\pm SEM) for five pulses (the third through seventh pulse in MK-801) is shown at the far right of each plot. *E*, Bars indicate mean \pm SEM for pooled data from $n = 8$ (NR1A/NR2A) or $n = 11$ (NR1A/NR2B) different cells. Significant difference by unpaired *t* test, $**p < 0.01$. *F*, The fraction of peak current blocked with each successive pulse of MK-801 plus glutamate ($1 - [I_N/I_{N-1}]$) was calculated from recordings made from $n = 5$ –11 cells, for each of five different MK-801 concentrations.

on a time scale of seconds (at hyperpolarized membrane potentials) to milliseconds (at depolarized potentials) and traps agonist in the bound state (Benveniste and Mayer, 1995), as evidenced by the slow decay of tail currents seen in Figure 7, *A* and *B*. These properties can be exploited to obtain a more quantitative estimate of the proportion of channels opening after the peak for the two subtypes. As previously reported (Benveniste and Mayer, 1995), a 500 msec pulse of 9-AA together with agonist applied at hyperpolarized potentials will result in accumulation of channels in the blocked agonist-bound state. Because the time constant for 9-AA unblock is < 3 msec at +60 mV, all of the agonist-bound channels that had accumulated in the blocked state will open nearly simultaneously after depolarization (Fig. 7*C,E,F,H*). Thus, the ratio of the peak amplitude of the agonist-evoked current response at +60 mV (Fig. 7*D,G*) to that of the tail current evoked by depolarization to +60 mV after 9-AA block (Fig. 7*C,F*) provides a rough estimate of the fraction of channels

open at the peak of the current response compared with the $P_{O(\text{total})}$ for the 500 msec agonist application (Benveniste and Mayer, 1995). This ratio is approximately twofold larger for NR1A/NR2A than NR1A/NR2B (0.72 ± 0.04 , $n = 6$ and 0.35 ± 0.02 , $n = 4$, respectively; $p < 0.01$ by unpaired *t* test; Fig. 7*I*), indicating that a larger fraction of channels open after the peak for NR1A/NR2B (65%) than for NR1A/NR2A (28%). Comparison of the decay phase of the outward current evoked by the +60 mV depolarization after 9-AA block to that of the agonist-evoked response revealed a similar time course for NR1A/NR2A (Fig. 7*E,J*). In contrast, the voltage-activated current (after 9-AA block) mediated by NR1A/NR2B exhibited a fast component, representing $\sim 68\%$ of the total peak with a time constant $\tau = 29 \pm 2$ msec ($n = 6$), that was not apparent in the decay of the agonist-evoked response; the remainder of the decay followed a similar time course to that exhibited by the agonist-evoked response (Fig. 7*H,K*). Together, these results suggest that peak P_o

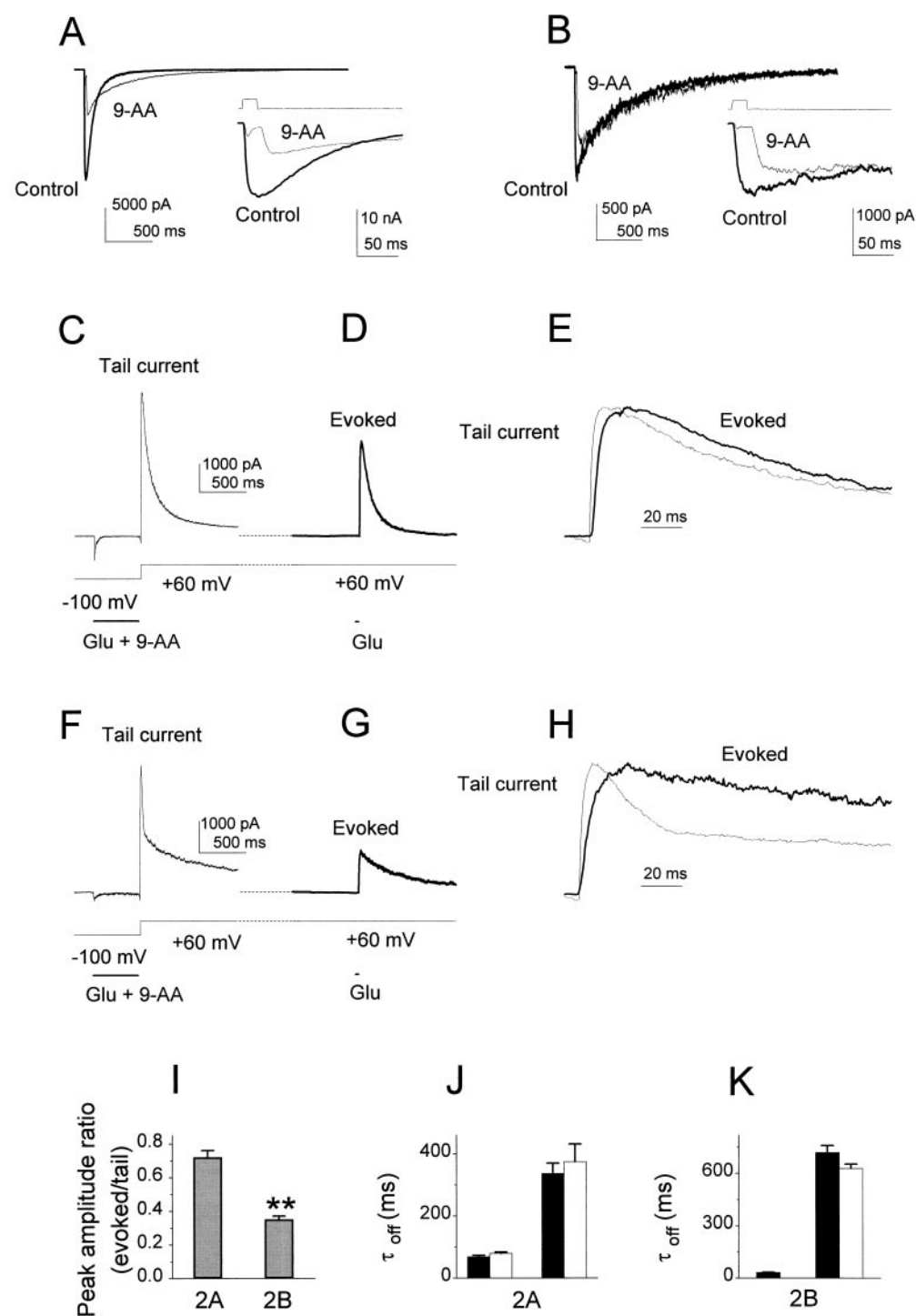


Figure 7. 9-aminoacridine block reveals larger fraction of channels open after the peak response for NR1A/NR2B than NR1A/NR2A. *A, B*, Representative traces showing NR1A/NR2A (*A*) or NR1A/NR2B (*B*) mediated current evoked by 20 msec application of 1 mM glutamate (Control, thick line) or 1 mM glutamate plus 100 μ M 9-AA (9-AA, thin line). Holding potential was -60 mV. The top trace in the inset is the open tip recording at the end of the experiment. *C–H*, Representative traces recorded from cell expressing NR1A/NR2A (*C–E*) or NR1A/NR2B (*F–H*). Current elicited by voltage switch from -100 to $+60$ mV 20 msec after a 500 msec application of 1 mM glutamate plus 100 μ M 9-AA (*C, F*, Tail current, thin lines). Current evoked by 20 msec application of 1 mM glutamate at a holding potential of $+60$ mV (*D, G*, Evoked, thick lines). *E* and *H* show same currents on expanded time scale and evoked current peaks are normalized to those of tail currents. *I–K*, Bars represent mean \pm SEM from $n = 6$ different cells for each subtype. *J* (for NR1A/NR2A) and *K* (for NR1A/NR2B) compare the time constant or constants of current decay for voltage-activated currents immediately after 9-AA application (filled bars) with those for glutamate-evoked currents (open bars), both obtained at holding potentials of $+60$ mV. $**p < 0.01$ by unpaired *t* test. Extracellular solution contained 0.2 mM calcium.

for NR1A/NR2B is significantly smaller than that for NR1A/NR2A at least in part because of a longer latency to first opening after saturation of receptors with agonist.

DISCUSSION

Our results demonstrate that the maximal channel open probability of NMDA receptors is dependent on subunit composition. According to differences in macroscopic peak current density and block by MK-801, peak P_o for NR1A/NR2A is twofold to fivefold higher than that for NR1A/NR2B. Previous studies using

10–20 μ M MK-801 to measure peak P_o for neuronal NMDA receptors have yielded results in the range of 0.04 to 0.3 (Jahr, 1992; Rosenmund et al., 1995; Dzubay and Jahr, 1996), and it has been suggested that peak P_o for NMDA receptor-mediated current responses may differ for recordings made in the whole-cell versus outside-out patch mode (Benveniste and Mayer, 1995; Rosenmund et al., 1995). Interestingly, our estimate of peak P_o , using a protocol and analysis from Jahr (1992), was 0.35 for NR1A/NR2A and 0.07 for NR1A/NR2B, values similar to the high and low estimates reported for neuronal NMDA receptors.

Moreover, the charge transfer time course for NR1A/NR2A-mediated whole-cell current that we observed in the presence of 20 μM MK-801 is in excellent agreement with that found by Jahr (1992) for NMDA receptors in outside-out patches from hippocampal neurons. In addition, our estimate of peak P_o for NR1A/NR2A matches the value reported for open probability within NR1A/NR2A superclusters in single-channel recordings from outside-out patches (Wyllie et al., 1998). Therefore, our results suggest that at least some of the variability in measurements of peak P_o for neuronal NMDA receptors may be caused by differences in receptor subunit composition.

In experiments in which 20 μM MK-801 was present in both control and agonist solutions, the percentage block of peak current and charge transfer after wash-out of MK-801 was similar for currents mediated by NR1A/NR2A and NR1A/NR2B. These results indicate that $P_{o(\text{total})}$ (~ 0.7) for the peak and deactivation phase in response to brief agonist stimulation is similar for the two subtypes. On the other hand, results of experiments in which MK-801 had access to channels only during the peak of the current response (Figs. 4–6) revealed distinct differences between NR1A/NR2A and NR1A/NR2B, consistent with significant differences in peak P_o . Assuming some forebrain neurons or synapses express predominantly NR2A or NR2B subunits, this latter protocol may prove a useful tool for determining neuronal NMDA receptor subunit composition.

The fact that $P_{o(\text{total})}$ is similar but peak P_o is approximately twofold to fivefold higher for NR1A/NR2A than for NR1A/NR2B suggests that NR1A/NR2B channels have longer latencies to first opening, lower opening frequency, shorter mean open times, or some combination of these. Experiments with 9-aminoacridine suggest that some of the difference in peak P_o is attributable to a smaller fraction of NR1A/NR2B channels opening within the first 20 msec after a jump into a saturating concentration of agonist compared with NR1A/NR2A. Because the 10–90% rise-time for the macroscopic current response is slightly, but significantly, longer for NR1A/NR2B, the peak of the distribution of latencies to first opening may be slightly shifted to longer times, but may also be broader than that of NR1A/NR2A. On the other hand, Colquhoun et al. (Edmonds and Colquhoun, 1992; Wyllie et al., 1998) have suggested that NMDA receptor-mediated macroscopic current responses to jumps into a saturating concentration of agonist can be approximated by the ensemble average of aligned superclusters (recorded as single-channel openings during steady-state exposure to low agonist concentrations), as long as opening latency is ignored. If so, our results from MK-801 and 9-AA experiments could also be explained if NR1A/NR2B channels exhibited longer duration superclusters and smaller intracluster channel open probability compared with NR1A/NR2A, similar to the comparison between NR1A/NR2D and NR1A/NR2A reported by Wyllie et al. (1998). Because some NR1A/NR2A and NR1A/NR2B channels may escape block on first opening (because of open times less than ~ 1 msec; see Wyllie et al., 1998), the subtype with lower opening frequency within the supercluster would show less peak current attenuation. As well, this line of reasoning could explain why increasing the on-rate of MK-801 (by increasing its concentration) had a larger effect on block of NR1A/NR2B peak current than that of NR1A/NR2A; as the channel blocking rate increased from $\sim 250 \text{ sec}^{-1}$ at 10 μM to $\sim 2500 \text{ sec}^{-1}$ at 100 μM MK-801 (Heuttner and Bean, 1988; Jahr, 1992), the fraction of first openings that escaped block would have markedly decreased. Clearly, a comparison of NR1A/NR2A and

NR1A/NR2B superclusters in single-channel recordings from transfected mammalian cell lines would help resolve these issues.

Results of experiments with the agonist-trapping, use-dependent antagonist 9-aminoacridine indicate that the fraction of channels open at the peak of the macroscopic current response is more than twofold higher for NR1A/NR2A than for NR1A/NR2B. The estimated fractions, 0.72 and 0.35, respectively, are much higher than the values calculated from the MK-801 experiments (0.35 and 0.07, respectively) and are likely to be overestimates of the actual peak open probability for several reasons (see also Benveniste and Mayer, 1995). First, 9-AA unblock is not instantaneous, so some of the blocked channels will not contribute to the peak of the tail current. Second, because 9-AA unblock occurs (slowly) even at hyperpolarized potentials, 9-AA will have already dissociated from some of the channels during the interval between removal of agonist/9-AA and switching voltage from -100 to $+60$ mV (Fig. 7C,F). Thus, the tail current peak amplitude underrepresents $P_{o(\text{total})}$ for the 500 msec application of agonist/9-AA. It is worth noting that agonist-trapping properties and dissociation rates of 9-AA have not been compared for NR1A/NR2A and NR1A/NR2B, and any differences between the subtypes in these parameters would alter the relative values of estimated peak P_o . However, by applying depolarizing voltage within 20 msec after offset of 9-AA, we have attempted to minimize the effect that differences in 9-AA dissociation rates might have on our results. Third, since a fraction of available channels may have opened very briefly or not at all during the 500 msec application of agonist/9-AA, $P_{o(\text{total})}$, as represented experimentally by the tail current amplitude, may be <1 . It is interesting to note that not only the peak amplitude but also the time course of current decay at $+60$ mV is markedly different for the tail compared with evoked currents mediated by NR1A/NR2B. The large proportion ($\sim 68\%$) of tail current decaying by the fast (29 msec) time constant, which is absent in the agonist-evoked response, is consistent with synchronized channel opening after 9-AA unblock and a low opening frequency of NR1A/NR2B agonist-bound channels.

In concluding that numbers of surface receptors were similar for NR1A/NR2A and NR1A/NR2B from data analyzing expression of NR1A, we assumed that: (1) Every surface receptor containing NR1A also contained NR2 subunit or subunits; (2) Complexes of NR1A with NR2A shared the same stoichiometry as those of NR1A with NR2B; and (3) All surface receptors were functional. The first assumption is supported by data indicating that NR1A subunits expressed heterologously in the absence of NR2 subunits show little or no surface expression (McIlhinney et al., 1996). Although we have not directly tested the second and third assumptions, the ratio of peak P_o for NR1A/NR2A to that of NR1A/NR2B measured from MK-801 block experiments was similar to that predicted by the difference in peak macroscopic current density for the two subtypes. Therefore, it is likely that our assumptions were valid and that expression of functional receptors at the surface of transfected HEK 293 cells was similar for NR1A/NR2A and NR1A/NR2B under our experimental conditions.

A variety of data indicate that at typical CNS synapses, the presynaptic release of a single quantum of glutamate results in saturation of binding to postsynaptic NMDA receptors (Clements et al., 1992; Tang et al., 1994; Tong and Jahr, 1994). Therefore, the NMDA receptor-mediated component of the EPSC amplitude is directly proportional to the density of postsynaptic

receptors and their open probability. Our results suggest that when expressed at equal density, postsynaptic NMDA receptors composed predominantly of NR1A/NR2A will mediate peak currents approximately fourfold larger than those mediated by receptors composed of NR1A/NR2B. In support of this conclusion, a recent study in rat brain frontal cortex showed that, after repeated electroconvulsive seizures, upregulation of NR2B expression (in the absence of any change in NR2A expression) was associated with an approximately threefold decrease in peak amplitude of NMDA-evoked currents recorded from pyramidal neurons (Hiroi et al., 1998). Another study in cultured rat cerebellar granule cells demonstrated a significant decrease in amplitude of NMDA-evoked calcium transients that correlated with BDNF-induced downregulation of NR2A without a change in NR1A and NR2B expression levels (Brandoli et al., 1998). Interestingly, the alteration in NMDA receptor subunit composition resulting from BDNF treatment was associated with decreased vulnerability to excitotoxic neuronal death.

Previous studies have demonstrated that NR1A/NR2B is the predominant NMDA receptor subtype expressed in cortex and hippocampus during early developmental stages (Monyer et al., 1994; Sheng et al., 1994) and that this receptor subtype mediates the markedly slower time course of EPSC decay found in immature versus mature neurons (Carmignoto and Vicini, 1992; Hestrin, 1992; Flint et al., 1997). Although these slow EPSCs would be optimized for temporal integration of nonsynchronous synaptic inputs, our results suggest that they would be smaller in amplitude than those typically found in mature cortical and hippocampal neurons. Moreover, in mature forebrain neurons that express both NR2A and NR2B, stimuli that induce a switch in the relative expression levels of these subunits would be expected to alter EPSC amplitude and trigger a long-lasting change in synaptic efficacy, perhaps mediating synaptic plasticity and altered vulnerability to excitotoxicity.

REFERENCES

- Benveniste M, Mayer ML (1995) Trapping of glutamate and glycine during open channel block of rat hippocampal neuron NMDA receptors by 9-aminoacridine. *J Physiol (Lond)* 483:367–384.
- Brandoli C, Sanna A, De Bernardi MA, Follesa P, Brooker G, Mocchetti I (1998) Brain-derived neurotrophic factor and basic fibroblast growth factor downregulate NMDA receptor function in cerebellar granule cells. *J Neurosci* 18:7953–7961.
- Bricecombe JC, Boeckman FA, Aizenman E (1997) Functional consequences of NR2 subunit composition in single recombinant *N*-methyl-D-aspartate receptors. *Proc Natl Acad Sci USA* 94:11019–11024.
- Carmignoto G, Vicini S (1992) Activity-dependent decrease in NMDA receptor responses during development of the visual cortex. *Science* 258:1007–1011.
- Chen C, Okayama H (1987) High efficiency transformation of mammalian cells by plasmid DNA. *Mol Cell Biol* 7:2745–2752.
- Chen N, Moshaver A, Raymond LA (1997) Differential sensitivity of recombinant *N*-methyl-D-aspartate receptor subtypes to Zinc inhibition. *Mol Pharmacol* 51:1015–1023.
- Chen N, Luo T, Wellington C, Metzler M, McCutcheon K, Hayden MR, Raymond LA (1999) Subtype-dependent modulation of NMDA receptor mediated currents by mutant huntingtin. *J Neurochem* 72:1890–1898.
- Clements JD, Lester RA, Tong G, Jahr CE, Westbrook GL (1992) The time course of glutamate in the synaptic cleft. *Science* 258:1498–1501.
- Dingledine R, Borges K, Bowie D, Traynelis SF (1999) The glutamate receptor ion channels. *Pharmacol Rev* 51:7–61.
- Dzubay J, Jahr CE (1996) Kinetics of NMDA channel opening. *J Neurosci* 16:4129–4134.
- Edmonds B, Colquhoun D (1992) Rapid decay of average single-channel NMDA receptor activations recorded at low agonist concentration. *Proc R Soc Lond B Biol Sci* 250:279–286.
- Ehlers MD, Zhang S, Bernhardt JP, Haganir RL (1996) Inactivation of NMDA receptors by direct interaction of calmodulin with the NR1 subunit. *Cell* 84:745–755.
- Flint AC, Maisch US, Weishaupt JH, Kriegstein AR, Monyer H (1997) NR2A subunit expression shortens NMDA receptor synaptic currents in developing neocortex. *J Neurosci* 17:2469–2476.
- Hestrin S (1992) Developmental regulation of NMDA receptor-mediated synaptic currents at a central synapse. *Nature* 357:686–689.
- Hessler NA, Shirke AM, Malinow R (1993) The probability of transmitter release at a mammalian central synapse. *Nature* 366:569–572.
- Hiroi N, Marek GJ, Brown JR, Ye H, Saudou F, Vaidya VA, Duman RS, Greenberg ME, Nestler EJ (1998) Essential role of the fos B gene in molecular, cellular, and behavioral actions of chronic electroconvulsive seizures. *J Neurosci* 18:6952–6962.
- Hollmann M, Boulter J, Maron C, Beasley L, Sullivan J, Pecht G, Heinemann SF (1993) Zinc potentiates agonist-induced currents at certain splice variants of the NMDA receptor. *Neuron* 10:943–954.
- Huettnner JE, Bean BP (1988) Block of *N*-methyl-D-aspartate-activated current by the anticonvulsant MK-801: selective binding to open channels. *Proc Natl Acad Sci USA* 85:1307–1311.
- Jahr CE (1992) High probability opening of NMDA receptor channels by L-glutamate. *Science* 255:470–472.
- Kohr G, Seeburg PH (1996) Subtype-specific regulation of recombinant NMDA receptor-channels by protein tyrosine kinases of the src family. *J Physiol (Lond)* 492:445–452.
- Krupp JJ, Vissel B, Heinemann SF, Westbrook GL (1996) Calcium-dependent inactivation of recombinant *N*-methyl-D-aspartate receptors is NR2 subunit specific. *Mol Pharmacol* 50:1680–1688.
- Krupp JJ, Vissel B, Heinemann SF, Westbrook GL (1998) N-terminal domains in the NR2 subunit control desensitization of NMDA receptors. *Neuron* 20:317–327.
- Krupp JJ, Vissel B, Thomas CG, Heinemann SF, Westbrook GL (1999) Interactions of calmodulin and alpha-actinin with the NR1 subunit modulate Ca^{2+} -dependent inactivation of NMDA receptors. *J Neurosci* 19:1165–1178.
- Legendre P, Rosenmund C, Westbrook GL (1993) Inactivation of NMDA channels in cultured hippocampal neurons by intracellular calcium. *J Neurosci* 13:674–684.
- Lu YM, Roder JC, Davidow J, Salter MW (1998) Src activation in the induction of long-term potentiation in CA1 hippocampal neurons. *Science* 279:1363–1367.
- McBain CJ, Mayer ML (1994) NMDA receptor structure and function. *Physiol Rev* 75:723–760.
- McIlhinney RAJ, Molnar E, Atack JR, Whiting PJ (1996) Cell surface expression of the human *N*-methyl-D-aspartate receptor subunit 1a requires the co-expression of the NR2A subunit in transfected cells. *Neuroscience* 70:989–997.
- Monyer H, Sprengel R, Schoepfer R, Herb A, Higuchi M, Lomeli H, Burnashev N, Sakmann B, Seeburg PH (1992) Heteromeric NMDA receptors: molecular and functional distinction of subtypes. *Science* 256:1217–1221.
- Monyer H, Burnashev N, Laurie DJ, Sakmann B, Seeburg PH (1994) Developmental and regional expression in the rat brain and functional properties of four NMDA receptors. *Neuron* 12:529–540.
- Price CJ, Rintoul GL, Baimbridge KG, Raymond LA (1999) Inhibition of calcium-dependent NMDA receptor current rundown by calbindin-D28k. *J Neurochem* 72:634–642.
- Raymond LA, Moshaver A, Tingley WG, Shalaby I, Haganir RL (1996) Glutamate receptor ion channel properties predict vulnerability to cytotoxicity in a transfected non-neuronal cell line. *Mol Cell Neurosci* 7:102–115.
- Rosenmund C, Westbrook GL (1993) Calcium-induced actin depolymerization reduces NMDA channel activity. *Neuron* 10:805–814.
- Rosenmund C, Feltz A, Westbrook GL (1995) Synaptic NMDA receptor channels have a low open probability. *J Neurosci* 15:2788–2795.
- Sheng M, Cummings J, Roldan LA, Jan YN, Jan LY (1994) Changing subunit composition of heteromeric NMDA receptors during development of rat cortex. *Nature* 368:144–147.

- Stern P, B     P, Schoepfer R, Colquhoun D (1992) Single-channel conductances of NMDA receptors expressed from cloned cDNAs: comparison with native receptors. *Proc R Soc Lond B Biol Sci* 250:271–277.
- Stern P, Cik M, Colquhoun D, Stephenson FA (1995) Single channel properties of cloned NMDA receptors in a human cell line: comparison with results from *Xenopus* oocytes. *J Physiol (Lond)* 476:391–297.
- Sucher NJ, Awobuluyi M, Choi YB, Lipton SA (1996) NMDA receptors: from genes to channels. *Trends Pharmacol Sci* 17:348–355.
- Sugihara H, Moriyoshi K, Ishii T, Masu M, Nakanishi S (1992) Structures and properties of seven isoforms of the NMDA receptor generated by alternative splicing. *Biochem Biophys Res Commun* 185:826–832.
- Tang CM, Margulis M, Shi QY, Fielding A (1994) Saturation of postsynaptic glutamate receptors after quantal release of transmitter. *Neuron* 13:1385–1393.
- Tong G, Jahr CE (1994) Block of glutamate transporters potentiates postsynaptic excitation. *Neuron* 13:195–203.
- Vicini S, Wang JF, Li JH, Zhu WJ, Wang YH, Luo JH, Wolfe BB, Grayson DR (1998) Functional and pharmacological differences between recombinant *N*-methyl-D-aspartate receptors. *J Neurophysiol* 79:555–566.
- Wang YT, Yu X-M, Salter MW (1996) Ca^{2+} -independent reduction of *N*-methyl-D-aspartate channel activity by protein tyrosine phosphatase. *Proc Natl Acad Sci USA* 93:1721–1725.
- Wyllie DJA, Behe P, Colquhoun D (1998) Single-channel activations and concentration jumps: comparison of recombinant NR1a/NR2A and NR1a/NR2D NMDA receptors. *J Physiol (Lond)* 510:1–18.
- Zhang S, Ehlers MD, Bernhardt JP, Su CT, Huganir RL (1998) Calmodulin mediates calcium-dependent inactivation of *N*-methyl-D-aspartate receptors. *Neuron* 21:443–453.